Numerical Solution of the Dam-Break Problem with a Discontinuous Galerkin Method

Sergio Fagherazzi[1]; Patrick Rasetarinera[2]; M. Youssuff Hussaini[3]; and David J. Furbish[4]

Abstract: A discontinuous Galerkin method for the solution of the dam-break problem is presented. The scheme solves the shallow water equations with spectral elements, utilizing an efficient Roe approximate Riemann solver in order to capture bore waves. The solution is enhanced by a projection limiter that eliminates spurious oscillations near discontinuities. The main advantage of the model is the flexibility in approximating smooth solutions with high-order polynomials and resolving at the same time discontinuous shock waves. Furthermore, the finite element discretization is capable of handling complex geometries and producing correct results near the boundaries. Both the *h*- and *p*-type extensions are investigated for the one-dimensional dam break, and the results are verified by comparison with analytical solutions. The application to a two-dimensional dam-break problem shows the efficiency and stability of the method.

DOI: 10.1061/(ASCE)0733-9429(2004)130:6(532)

CE Database subject headings: Shallow water; Floods; Dams; Numerical models; Shock waves; Finite element method.

Introduction

In recent years, several new numerical methods have been developed to solve systems of hyperbolic equations. A typical example of a hyperbolic system is the shallow water equations utilized in modeling fluid flow in rivers and estuaries. The solution of hyperbolic equations is complicated by the fact that, under particular conditions, they lead to discontinuous solutions. This is the case of the break of a dam in a river, in which the sudden dam collapse produces a bore of finite amplitude (shock) traveling at fast speed in the domain.

Common computational techniques utilized to solve the shallow water equations are based on finite difference methods that solve the differential form of the shallow water equations (Leendertse 1967; Abbot et al. 1973). These methods, however accurate where the solution is smooth, are not suitable to solve the hyperbolic equations near discontinuities (shock waves). Recent methods, which can be named shock-capturing high-resolution schemes, compute flow discontinuities sharply and without oscillations. These methods solve the shallow water equations in integral form, keeping in account, in that way, discontinuous solutions. To increase the resolution of discontinuities, the incorporation of the physical properties of wave propagation is necessary, as is, in particular, the solution of the Riemann problem springing between two nodes or elements with a jump in the values of the variables. These methods can be developed on Cartesian grids (Toro 1992; Zoppou and Roberts 2000) or through a finite volume discretization (Alcrudo and Garcia-Navarro 1993; Zhao et al. 1994; Mingham and Causon 1998), where the latter increases the flexibility in dealing with boundary conditions and complex flow geometries.

In each of these methods, the link between two nodes takes place with an approximate Riemann solver. Particularly effective are the HLL flux method (Harten et al. 1983) utilized in Mingham and Causon (1998), the Roe approximate Riemann solver (Roe 1981) utilized in Alcrudo and Garcia-Navarro (1993) and Jha et al. (1995), and the weighted average flux (WAF) introduced by Toro (1989) and utilized in Zoppou and Roberts (2000), Toro (1992), and Fraccarollo and Toro (1995). Higher-order methods often present oscillations near discontinuities that can be eliminated through suitable flux or slope limiters, which have to be incorporated in the finite difference or finite volume formulation. Examples are van Leer's monotonic upstream schemes (MUSCL) approach (van Leer 1974) applied in Alcrudo and Garcia-Navarro (1993) and Mingham and Causon (1998), and the SUPERBEE (Roe 1985) and the MINIMOD [see Hirsch (1989)], both applied in Fraccarollo and Toro (1995).

At the same time, far from discontinuities, the solution can be smooth and suitable for calculation with high-order approximating polynomials, i.e., spectral methods (Canuto et al. 1988; Fornberg 1996).

Discontinuous Galerkin methods [see Cockburn et al. (2000) for a review] are then optimal candidates for the solution of complex problems such as the dam break. These methods couple a discontinuous spatial discretization involving flux balances across the interfaces of the elements (technique at the base of shock-capturing schemes) with a high-order polynomial approximation inside each element.

The weak formulation of the equations and the discontinuous polynomial basis lead to an accurate representation of bore waves (shocks). At the same time, the spectral approximation increases the convergence where the solution is smooth, allowing the use of fewer computational nodes. Finally, the discretization of the do-

[1]Assistant Professor, Dept. of Geological Sciences and School of Computational Science and Information Technology, Florida State Univ., Tallahassee, FL 32306-4120.

[2]Research Assistant, School of Computational Science and Information Technology, Florida State Univ., Tallahassee, FL 32306-4120.

[3]Professor, School of Computational Science and Information Technology, Florida State Univ., Tallahassee, FL 32306-4120.

[4]Professor, Dept. of Geological Sciences, Tallahassee, FL 32306.

Note. Discussion open until November 1, 2004. Separate discussions must be submitted for individual papers. To extend the closing date by one month, a written request must be filed with the ASCE Managing Editor. The manuscript for this paper was submitted for review and possible publication on March 8, 2002; approved on December 3, 2003. This paper is part of the ***Journal of Hydraulic Engineering***, Vol. 130, No. 6, June 1, 2004. ©ASCE, ISSN 0733-9429/2004/6-532–539/$18.00.

main in finite elements is extremely effective in modeling complex geometries.

In this paper, a discontinuous Galerkin method, the RKDG method (Bassi and Rebay 1997; Cockburn and Shu 1998), is utilized to solve the dam-break problem [see also Schwanenberg and Kongeter (2000)]. The method applies an explicit Runge-Kutta time discretization and is highly parallelizable. High-order polynomials inside each segment in 1D or each quadrilateral in 2D are utilized. The elements are connected through numerical fluxes expressed as an approximate Riemann solver (Roe numerical flux), and a projection limiter prevents oscillations near solution discontinuities (Biswas et al. 1994). The method is applied to the classical one-dimensional problem. In the part of the domain where the shock is not present (reservoir), two convergence analyses for *h* refinement (increasing the number of elements) and *p* refinement (increasing the order of the polynomials utilized in each element) are performed. In the part where the shock is present (tailwater), the limiter prevents the formation of oscillations and only the *h*-type extension is studied. The method is then applied to a two-dimensional dam-break problem where its flexibility can suitably model the complex geometry of the system.

Discontinuous Galerkin Formulation

To illustrate the discontinuous Galerkin method, the conservation form of the two-dimensional shallow water equations is considered

$$\frac{\partial \mathbf{U}}{\partial t}+\frac{\partial \mathbf{F}}{\partial x}+\frac{\partial \mathbf{G}}{\partial y}=0 \tag{1}$$

with

$$\mathbf{U}=\begin{bmatrix}\phi\\ \phi u\\ \phi w\end{bmatrix},\quad \mathbf{F}=\begin{bmatrix}\phi u\\ \phi u^2+\frac{1}{2}\phi^2\\ \phi uw\end{bmatrix},\quad \mathbf{G}=\begin{bmatrix}\phi w\\ \phi uw\\ \phi w^2+\frac{1}{2}\phi^2\end{bmatrix} \tag{2}$$

where $\phi=gh$; $\mathbf{v}=(u,w)$ is the velocity vector; g=gravity acceleration; and h=water depth. In Eq. (1), a flat bottom surface is assumed and bottom friction is neglected [for a complete description of the shallow waters equations, see Dronkers (1964)].

To compute an approximate solution $\mathbf{U}_h$ of Eq. (1), the domain is partitioned into nonoverlapping quadrilaterals E_i. In each element E_i, $\mathbf{U}_h$ is written as a polynomial expansion

$$\mathbf{U}_h^i(\mathbf{x},t)=\sum_{k=0}^{K}\hat{U}_k^i(t)\Psi_k(\mathbf{x}),\quad \mathbf{x}\in E_i \tag{3}$$

where the basis functions Ψ_k=polynomials; K=number of degrees of freedom in the element E_i (i.e., the number of collocation points); and $\hat{U}_k^i$=degrees of freedom that are computed by solving a weak formulation of Eq. (1)

$$\int_{E_i}\frac{\partial \mathbf{U}_h^i}{\partial t}\Psi_k\,d\mathbf{x}+\int_{E_i}\left(\frac{\partial \mathbf{F}_h}{\partial x}+\frac{\partial \mathbf{G}_h}{\partial y}\right)\Psi_k\,d\mathbf{x}=0$$
$$k=0,...,K \tag{4}$$

with $\mathbf{F}_h=\mathbf{F}(\mathbf{U}_h^i)$ and $\mathbf{G}_h=\mathbf{G}(\mathbf{U}_h^i)$. Using Green's formulas, Eq. (4) is recast as

$$\int_{E_i}\frac{\partial \mathbf{U}_h^i}{\partial t}\Psi_k\,d\mathbf{x}-\int_{E_i}\left(\mathbf{F}_h\frac{\partial \Psi_k}{\partial x}+\mathbf{G}_h\frac{\partial \Psi_k}{\partial y}\right)d\mathbf{x}$$
$$+\int_{\partial E_i}(\mathbf{F}_h n_1+\mathbf{G}_h n_2)\Psi_k\,d\Gamma=0,\quad k=0,...,K \tag{5}$$

where ∂E_i=boundary of E_i and $\mathbf{n}=(n_1,n_2)$ denotes the unit outward normal vector. The third term in Eq. (5) is the integral of the function $(\mathbf{F},\mathbf{G})$ on the element boundary and represents the flux of the conserved variables (momentum and water volume) outside (or inside) the element. This term is the only connection between two contiguous elements and allows the construction of the solution within the domain. Since the conserved quantities are in general discontinuous across the interfaces of contiguous elements, we replace the flux $(\mathbf{F}_h n_1+\mathbf{G}_h n_2)$ with a numerical flux $\mathbf{H}$ that is an approximation of the real flux on the edges of the mesh elements. Clearly the numerical flux will be a function of the conserved variables at the left and at the right of each edge, but, instead of taking a simple average of the two values, a suitable Riemann solver is utilized to capture the wave properties of the solution. The numerical flux is thus the determinant factor for a correct approximation of discontinuous solutions.

If $\mathbf{U}_h^i$ and $\mathbf{U}_h^j$ are the values of the conserved variables at the inside and outside interface of the element, the numerical flux $\mathbf{H}$ can be defined as

$$(\mathbf{F}_h n_1+\mathbf{G}_h n_2)|_{\partial E_i}=\overline{\mathbf{H}}(\mathbf{U}_h^i,\mathbf{U}_h^j,\mathbf{n}) \tag{6}$$

To evaluate Eq. (5), it is convenient to map the element E_i into the reference square $[-1,1]\times[-1,1]$. The integrals in Eq. (5) are then computed using the Gauss quadrature formula

$$\int_{-1}^{1}f(\xi)d\xi=\sum_{k=0}^{N}f(\xi_k)\omega_k\int_{-1}^{1}\int_{-1}^{1}f(\xi,\eta)d\xi\,d\eta$$
$$=\sum_{k,l=0}^{N}f(\xi_k,\eta_1)\omega_k\omega_1 \tag{7}$$

that is exact for polynomials f of order up to $2N+1$. Here ξ_k=Gauss-Legendre collocation nodes associated with the weight ω_k [see Canuto et al. (1988) for a detailed description]. Using a tensor product of the Lagrange interpolating polynomials as basis functions, the approximate solution (3) in E_i reads

$$\mathbf{U}_h^i(\xi,\eta)=\sum_{k=0}^{N}\sum_{l=0}^{M}\hat{U}_{k,l}^i L_k(\xi)L_1(\eta)(\xi,\eta)\in[-1,1]\times[-1,1] \tag{8}$$

with $\hat{U}_{k,l}^i=\mathbf{U}_h^i(\xi_k,\eta_1)$ and L_k=Lagrange polynomial of order k. N and M are the number of collocation points in the x and y directions, respectively, so that the total number of degrees of freedom is $K=N\times M$. Hence, from Eq. (5), K equations for the nodal values of the solution at the Legendre quadrature points (also called collocation points) are obtained.

To complete the method, an explicit third-order TVD Runge-Kutta scheme (Shu and Osher 1988) is used to discretize the temporal derivative in Eq. (5). The time step Δt is then restricted by a Courant-Friedrichs-Levy condition

$$\Delta t\leq c_1\min\left(\frac{h_{\min}^i}{C_{\max}^i\max(1,N^2,M^2)}\right) \tag{9}$$

J. Hydraul. Eng., 2004, 130(6): 532-539

where $h^i_{\min}$=length of the smallest edge of E_i and $C^i_{\max}$=maximum, in absolute value, of the wave speeds in E_i. For the shallow water equations we have

$$C_{\max}=\max(|\sqrt{u^2+w^2}+\sqrt{\phi}|,|\sqrt{u^2+w^2}-\sqrt{\phi}|) \tag{10}$$

The constant c_1 depends on the order of the Runge-Kutta method implemented and on the order N and M of the polynomial basis in the x and y directions, respectively. In the present study, this constant is set to $c_1=0.5$.

Roe Numerical Flux

The choice of the numerical flux in Eq. (6) is important because it determines the properties of the method. The computation of the numerical flux (6) has been the subject of several works in recent years (Toro 1992). In the present paper, we use the Roe numerical flux that is often utilized in finite-difference and finite-volume methods.

The Roe numerical flux function is given by

$$\overline{\mathbf{H}}(\mathbf{U}^i,\mathbf{U}^j,\mathbf{n})=\frac{1}{2}[\mathbf{H}(\mathbf{U}^i)+\mathbf{H}(\mathbf{U}^j)]-|\overline{\mathbf{A}}|(\mathbf{U}^i-\mathbf{U}^j) \tag{11}$$

where $\mathbf{H}=\mathbf{F}n_1+\mathbf{G}n_2$ and $\overline{\mathbf{A}}=\partial\mathbf{H}/\partial\mathbf{U}$ is the Roe matrix that is the Jacobian matrix of the projection of the flux in the normal direction $\mathbf{n}$, evaluated at some average state to satisfy the relationship

$$\mathbf{H}(\mathbf{U}^i)-\mathbf{H}(\mathbf{U}^j)=\overline{\mathbf{A}}(\mathbf{U}^i-\mathbf{U}^j) \tag{12}$$

In Eq. (11), the matrix $|\overline{\mathbf{A}}|$ introduces numerical viscosity that artificially smears discontinuities.

For the two-dimensional shallow water equations $\overline{\mathbf{A}}$ is

$$\overline{\mathbf{A}}=\begin{pmatrix} 0 & n_1 & n_2 \\ (\overline{c}^2-\overline{u}^2)n_1-\overline{uw}n_2 & 2\overline{u}n_1+\overline{v}n_2 & \overline{u}n_2 \\ -\overline{uw}n_1+(\overline{c}^2-\overline{w}^2)n_2 & \overline{w}n_2 & \overline{u}n_1+2\overline{v}n_2 \end{pmatrix} \tag{13}$$

where $c=\sqrt{\phi}$ and

$$\overline{w}=\frac{c_iw_i+c_jw_j}{c_i+c_j}$$

$$\overline{u}=\frac{c_iu_i+c_ju_j}{c_i+c_j} \tag{14}$$

$$\overline{c}=\sqrt{\frac{1}{2}(c_i^2+c_j^2)}$$

To evaluate the flux (11), $|\overline{\mathbf{A}}|$ is computed as

$$|\overline{\mathbf{A}}|=R|\Lambda|R^{-1} \quad \text{with} \quad \overline{\mathbf{A}}=R\Lambda R^{-1} \tag{15}$$

Here R is the matrix of the right eigenvectors of $\overline{\mathbf{A}}$

$$R=\begin{pmatrix} \frac{1}{2}+(\overline{\mathbf{v}}\cdot\mathbf{n})/2\overline{c} & -n_1/2\overline{c} & -n_2/2\overline{c} \\ \overline{w}n_1-un_2 & n_2 & -n_1 \\ \frac{1}{2}-(\overline{\mathbf{v}}\cdot\mathbf{n})/2\overline{c} & n_1/2\overline{c} & n_2/2\overline{c} \end{pmatrix}$$

$$R^{-1}=\begin{pmatrix} 1 & 0 & 1 \\ \overline{u}-\overline{c}n_1 & n_2 & \overline{u}+\overline{c}n_1 \\ \overline{w}-\overline{c}n_2 & -n_1 & \overline{w}+\overline{c}n_2 \end{pmatrix} \tag{16}$$

and $\Lambda=\text{diag}(\overline{\mathbf{v}}\cdot\mathbf{n}-\overline{c},\overline{\mathbf{v}}\cdot\mathbf{n},\overline{\mathbf{v}}\cdot\mathbf{n}+\overline{c})$ is a diagonal matrix whose entries are the eigenvalues of $\mathbf{A}$.

Projection Limiting

Because of the polynomial representation (3) of the solution, the presence of discontinuities might cause spurious oscillations when high-order polynomials are used. To avoid these nonphysical oscillations, a limiting procedure developed in Biswas et al. (1994) is performed before each Runge-Kutta stage. For the sake of simplicity, we first describe the method for the one-dimensional case.

First, the Legendre coefficients of the solution in each element E_i are computed as

$$\alpha^i_k=\frac{\int^1_{-1}\mathbf{U}^i_h(\xi)l_k(\xi)d\xi}{\int^1_{-1}l^2_k(\xi)d\xi}, \quad k=0,\ldots,N \tag{17}$$

where l_k=Legendre polynomial of order k (Canuto et al. 1988).

Then, for $k=N,\ldots,1$ the coefficients α^i_k of each element E_i are limited using

$$(2k+1)\alpha^i_{k+1}=\text{minmod}((2k+1)\alpha^i_{k+1},\alpha^{i+1}_k-\alpha^i_k,\alpha^i_k-\alpha^{i-1}_k) \tag{18}$$

with

$$\text{minmod}(a,b,c)=\begin{cases}\text{sgn}(a)\min(|a|,|b|,|c|) & \text{if } \text{sgn}(a)=\text{sgn}(b)=\text{sgn}(c)\\ 0 \quad \text{otherwise}\end{cases} \tag{19}$$

It must be noted that the coefficients α_k are limited for all the elements before the coefficients α_{k-1}. The limited solution in each element E_i is then

$$\mathbf{U}^i_h(\xi)=\sum_{k=0}^{N}\alpha^i_kl_k(\xi) \tag{20}$$

For the two-dimensional case, the Legendre coefficients in the element E_i are computed as

$$\alpha^i_{k,l}=\frac{\int^1_{-1}\int^1_{-1}\mathbf{U}^i_h(\xi,\eta)l_k(\xi)l_1(\eta)d\xi\,d\eta}{\int^1_{-1}l^2_k(\xi)l^2_1(\eta)d\eta\,d\xi}, \quad k,l=0,\ldots,N \tag{21}$$

where coefficients $\{\alpha_{k,0}\}_{k=N,\ldots,1}$ and $\{\alpha_{0,l}\}_{l=N,\ldots,1}$ are limited using the one-dimensional procedure in the x direction and y direction, respectively. The limited solution in the element E_i is given by

$$\mathbf{U}^i_h(\xi,\eta)=\sum_{k,l=0}^{N}\alpha^i_{k,l}l_k(\xi)l_1(\eta) \tag{22}$$

A better accuracy may be obtained when the limiter (18) is applied to the Legendre coefficients of the characteristic variables $\gamma=R^{-1}\mathbf{U}$ where the matrix R is evaluated using the average values of U in each element. Operatively the limiting procedure is implemented as follows: (1) first the variables (water height and discharges) are transformed in the characteristic variables with a matrix multiplication $\gamma=R^{-1}\mathbf{U}$; (2) the Legendre coefficients of the solution in each element are then calculated with Eq. (21); (3) the coefficients are modified (limited) applying Eqs. (18) and (19) first in the x and then in the y direction; (4) the limited solution expressed in terms of the original variables is finally reconstructed multiplying the characteristic variables by R ($\mathbf{U}=R\gamma$).

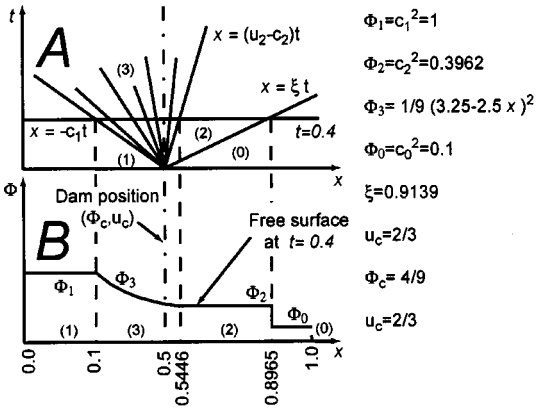

Fig. 1. One-dimensional dam break. (A) Characteristic lines in the x-t plane; (B) water levels. Numerical values describe the exact solution at time $t=0.4$.

One-Dimensional Dam Break

In the first numerical test, the one-dimensional dam break is solved in the domain [0,1]. At the beginning of the simulation, a dam divides the domain in two parts: the reservoir at the left and the tailwater at the right. The initial conditions are

$$\phi(x,0)=\begin{cases}\phi_L=1.0, & 0\leqslant x\leqslant \frac{1}{2}\\ \phi_R=0.1, & \frac{1}{2}<x\leqslant 1\end{cases} \tag{23}$$

$$u(x,0)=0, \quad x\in[0,1] \tag{24}$$

The dam is instantaneously removed and the solution computed in time until $t=0.4$. The exact solution for this problem can be found in Stoker (1957) and Wu et al. (1999). Using the characteristic lines [Fig. 1(A)], the corresponding water levels are calculated [Fig. 1(B)]. The critical depth and the critical velocity establish at the dam location, and do not vary during the entire simulation. In the reservoir, a rarefaction wave propagates to the left, whereas in the tailwater a shock wave forms and propagates to the right (Fig. 1). The application of the Hugoniot conditions allows us to analytically find the shock height and speed (Stoker 1957).

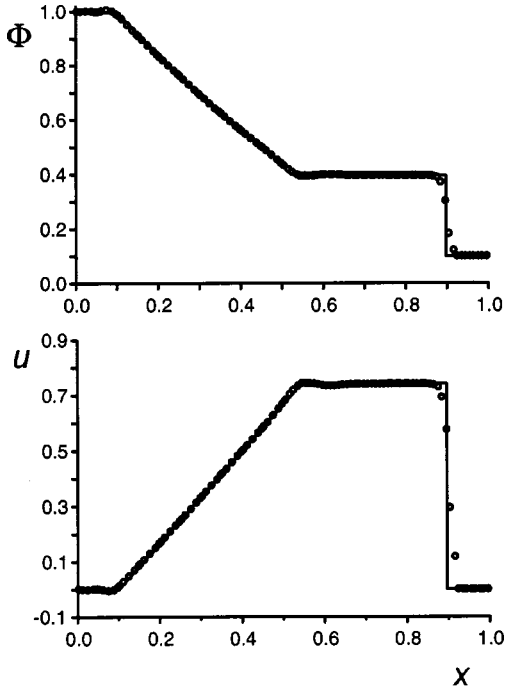

Fig. 2. Numerical solution (circles) and exact solution (line) of dam-break problem at time $t=0.4$. In the left part (reservoir) polynomials of order 4 with a filter are used; in the right part (tailwater) polynomials of order 1 with a slope limiter capture the bore.

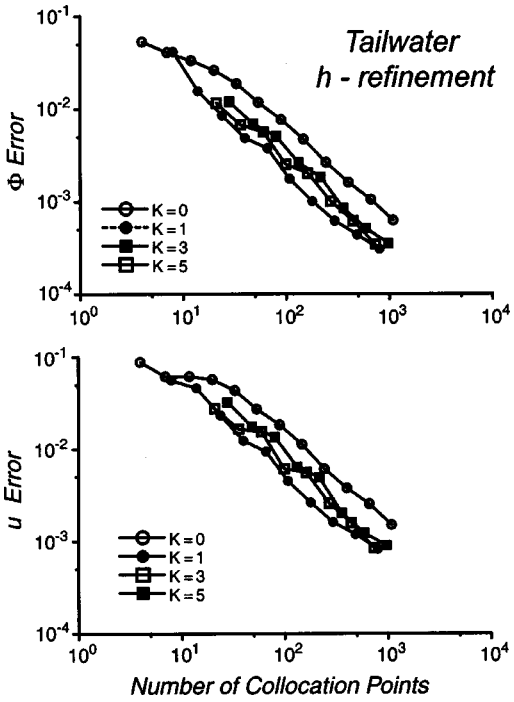

Fig. 3. Convergence analysis for the h-type extension in the tailwater. The number of collocation points is increased by augmenting the number of elements. For each curve, polynomial order k is fixed.

In the numerical simulation, the domain is descritized using 100 collocation nodes, 50 in the left and 50 in the right part. In the tailwater region, the domain is divided into 25 elements, each containing two collocation points ($N=1$, order 1 polynomial basis); the projection limiting procedure is applied in this region in order to avoid oscillations due to the shock discontinuity. In the reservoir, we use 10 elements each containing five collocation points ($N=4$, order 4 polynomial basis). As we can see in Fig. 2, the solution is free of oscillations near the discontinuity and the shock wave is resolved with two to four collocation points. We can directly compare the discontinuous Galerkin solution with the high-resolution finite volume method utilized in Toro (1992). The solution shown in Fig. 14 of Toro (1992) was calculated, with the same number of mesh points, utilizing the WAF method with the TS approximate Riemann solver and the TVD function SUPERA [see Toro (1992) for the method implementation]. We note that the high-resolution method utilized by Toro (1992) has a sharper shock representation. This is because the shock occupies at least one element and the elements in the discontinuous Galerkin method are larger, or contain more points, than the elements in finite-volume methods. On the other hand, the solution in the left half of the domain is more accurate, with low dissipation and good resolution of the rarefaction wave due to the high order of the polynomials utilized.

J. Hydraul. Eng., 2004, 130(6): 532-539

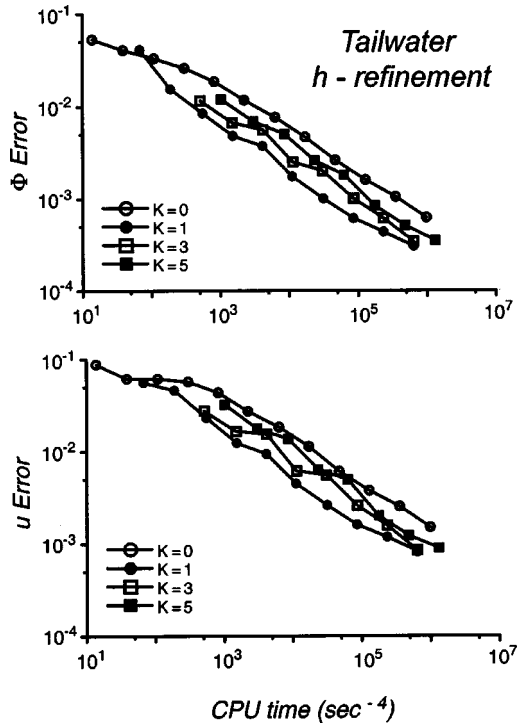

Fig. 4. CPU time with respect to the error for *h*-type extension in the tailwater; *k* is the order of the polynomials utilized

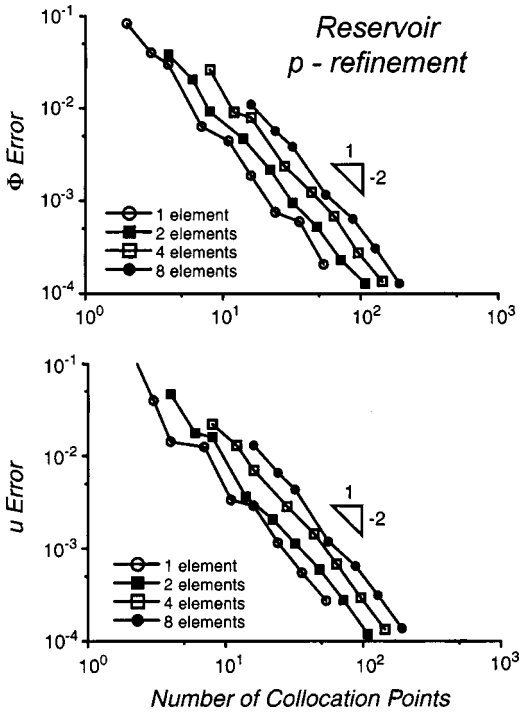

Fig. 6. Convergence analysis for the *p*-type extension in the reservoir. The number of collocation points is increased by augmenting the order of the polynomials inside each element. For each curve, the number of elements is fixed.

To show the convergence properties of the discontinuous Galerkin method, an error analysis using different refinement strategies is presented. To this end, the domain is split in two parts and each part is studied separately. The right part corresponds to the domain [1/2,1] and a constant critical water height and critical velocity are imposed at the left boundary. At $t=0$, the initial condition is $\phi=0.1$ and $u=0$. In the left part [0,1/2], the flow is subcritical and $\phi=1$ is imposed at $x=0$ while the critical height is imposed at $x=1/2$. The errors are measured using the discrete L_1 norm computed at the collocation points

$$Error=\|E\|_1=\frac{\Sigma_{j=0}^{N}|U_j-u_j|}{N+1} \tag{25}$$

where U_j=numerical solution at the point j and u_j=exact solution at the same point. The simulations were carried out with a SGI Origin 200 with 180 MHz CPU computer.

Fig. 3 shows the convergence rate of the solution in the right domain when an *h*-refinement strategy is used, i.e., the number of elements in the discretization is increased while the order of the polynomial basis in each element remains the same. Four curves are plotted, each corresponding to a different order of the polynomial basis ($N=0,1,3,5$, respectively). The error is plotted against the total number of collocation points. The results show that the approximation with first-order polynomials ($N=1$) leads to the best convergence rate. On one hand, the use of constant basis functions ($N=0$) causes high diffusion, smoothing both the shock and the rarefaction wave; on the other hand, the utilization of polynomials with order greater than 2 is counterproductive because the limiter lowers the order of the numerical approximation to 1 near the shock. Even a comparison of the CPU time needed to reach the numerical solution with a predetermined error is favorable to the use of a first-order polynomial basis (Fig. 4). The time step utilized in these simulations is derived from Eq. (9).

In the reservoir, we know that a rarefaction wave is present without shocks. The lack of discontinuities in the solution allows us to study both *h*- and *p*-type refinements without the projection limiting procedure.

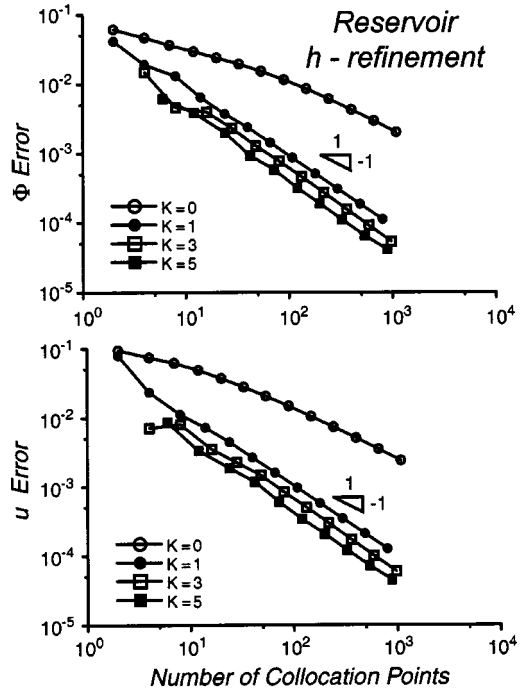

Fig. 5. Convergence analysis for the *h*-type extension in the reservoir. The number of collocation points is increased by augmenting the number of elements. For each curve, polynomial order *k* is fixed.

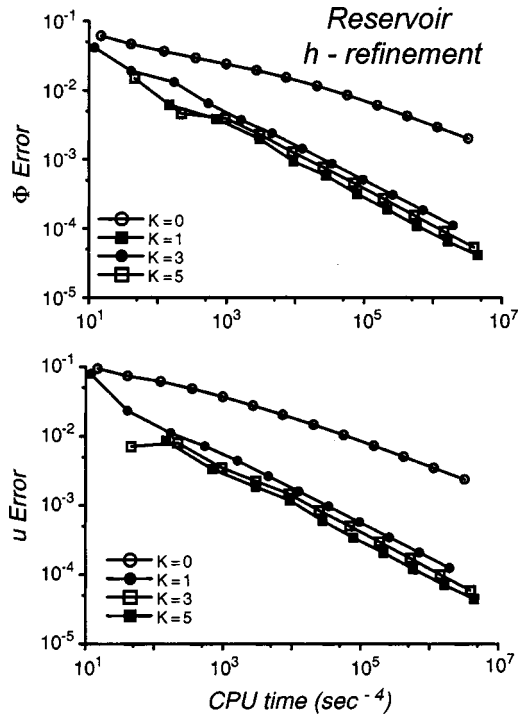

Fig. 7. CPU time with respect to the error for *h*-type extension in the reservoir; *k* is the order of the polynomials utilized

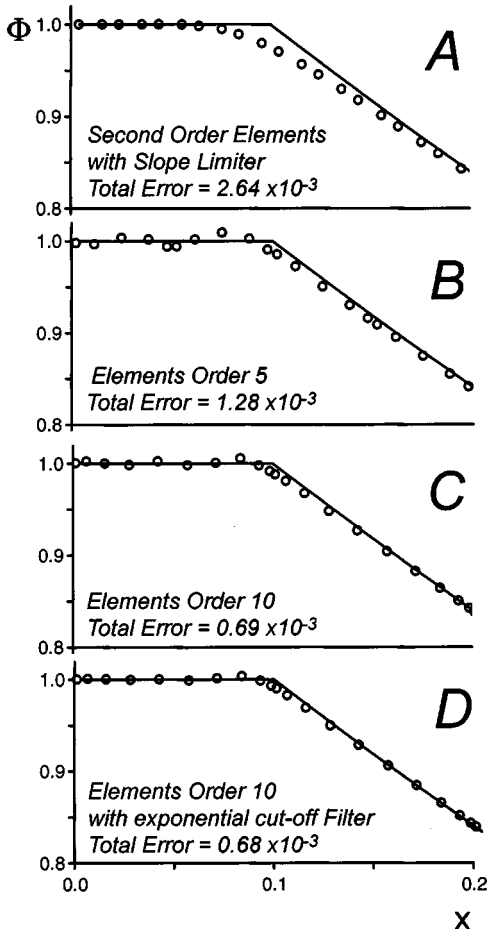

Fig. 8. Detailed comparison of numerical solution (circles) and exact solution (line) near point $x=0.1$

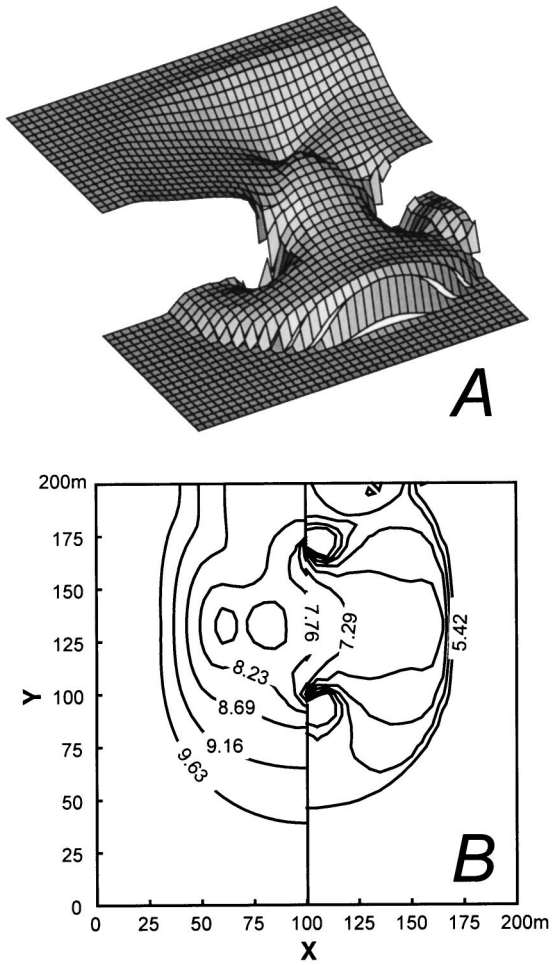

Fig. 9. Two-dimensional dam-break problem solved with a uniform square grid. Each element has four collocation points (order 2×2): (A) water surface 7.2 s after break of dam, (B) contour plot of water depth.

The error obtained with the *h*-type refinement is plotted as a function of the number of collocation points in a bilogarithmic plot, so that the slope of the curve indicates the convergence rate of the method (Fig. 5). Since the solution has a discontinuity in the first derivative, we found that the convergence rate is at most equal to 1 even with high-order polynomials (Fig. 5). In the *p*-type refinement, the number of elements is maintained constant and the number of collocation points is increased by augmenting the polynomial order in each element. The convergence rate of the method is found to be close to 2, i.e., double that with the *h* refinement (Fig. 6). Similar results have been found for the *h*-*p* extension of the finite element method applied to the Helmholtz equation (Babuska and Suri 1994).

These results confirm that, given a fixed number of collocation points, it is preferable to choose few elements with high-order polynomials than several elements with low-order polynomials for smooth solutions. The utilization of high-order polynomials is convenient even when comparing the processor time for the simulation, and that despite the demanding CFL condition (9) for the time step (Fig. 7).

To show the superiority of the approximation with high-order polynomials, we focus our attention on the point $x=0.1$ in the

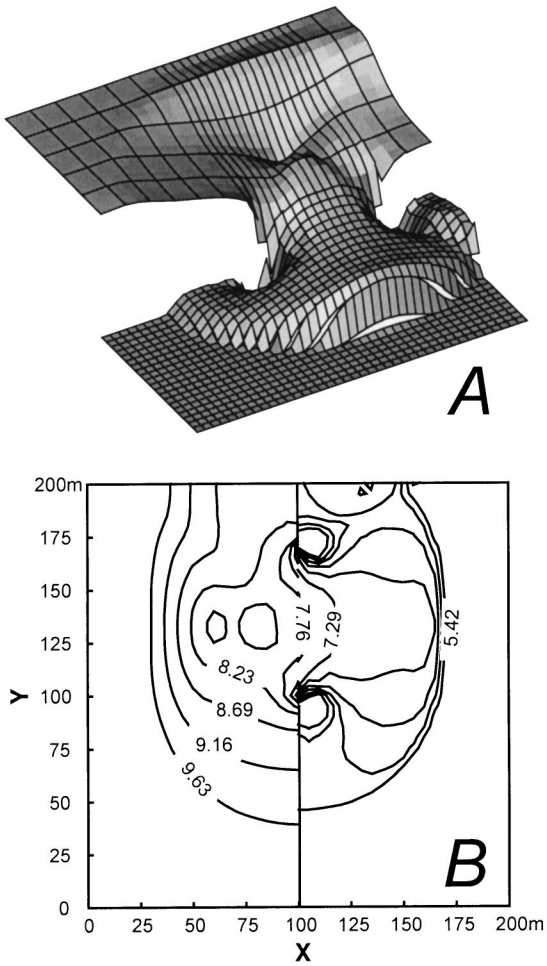

Fig. 10. Two-dimensional dam-break problem solved with high-order elements in the reservoir. Rectangular elements have twelve or eight collocation points (order 3×4 and 2×4): (A) water surface 7.2 s after break of dam, (B) contour plot of water depth.

reservoir at time $t=0.4$. Although oscillations due to the discontinuity in the first derivative are present, the solution with polynomials of order 9 [Fig. 8(C)] is closer to the exact solution than the solutions with lower polynomial order [Figs. 8(A) and 8(B)]. The solution can be enhanced utilizing an exponential cutoff filter (Majda et al. 1978) [Fig. 8(C)].

When combining the left and the right part, the time step Δt must be identical in each element. A higher-order approximation in the left part, leading to a small time step, automatically slows down the computation in the right part, so that polynomial bases of order lower or equal to 4 are preferred.

Two-Dimensional Dam Break

In this section, the discontinuous Galerkin method is applied to a two-dimensional dam-break problem. The geometry of the computational domain coincides with the example reported in Fennema and Chaudhry (1990), Alcrudo and Garcia-Navarro (1993), and Ambrosi (1995). A dam is located in the middle of a square domain of dimensions 200×200 m. At the beginning of the simulation, the water level inside the reservoir is equal to 10 m and the level of the water in the tailgate is 5 m. When the dam collapses, the water invades the tailgate [Fig. 9(A)].

The simulations were performed on two different grids. The first grid is uniform with 40×40 square elements and first-order polynomial functions in each element. The projection limiting procedure is applied in the tailgate region to avoid the nonphysical oscillations due to the shock discontinuity. Fig. 9(B) shows the computed solution at $t=7.2$ s. We can see that the shock front is sharply captured by the scheme. The second grid is nonuniform, with larger rectangular elements and high-order polynomial bases in the reservoir (Fig. 10). Although the second grid has fewer collocation points, the solution computed on both grids is identical, showing the flexibility of the discontinuous Galerkin method.

Conclusions

The discontinuous Galerkin method is particularly suitable to model systems of hyperbolic equations. In the dam break problem, the nonlinear character of the shallow water equations is responsible for the formation of a bore wave that propagates a finite speed in the computational domain. The weak formulation and the discontinuous bases utilized in the discontinuous Galerkin method are straightforward in treating such shock waves. At the boundaries of each element the fluxes are resolved by Roe approximate Riemann solvers, which keep in account the physics of the wave propagation. A slope limiter eliminates the spurious oscillations always present near shock fronts when using high order methods. At the same time, far from discontinuities in the flow field, it is possible to increase the polynomial order in the elements, achieving higher accuracy. Numerical results show that the method is stable without oscillations near the shock front for 1D and 2D problems. At the same time, an error analysis proves that where the shock is not present, i.e., in the reservoir, an exponential convergence rate is ensured by means of high order polynomials. In zones where the solution is smooth, a *p* refinement, increasing the order of the polynomials inside the elements, is thus more convenient than an *h* refinement, i.e. increasing the number of elements.

Notation

The following symbols are used in this paper:

$\mathbf{A}$ = Roe matrix;
E_i = element i of domain;
$\mathbf{F},\mathbf{G}$ = flux function in the x and y directions;
$\mathbf{F}_h,\mathbf{G}_h$ = flux function approximations;
g = gravity acceleration;
$\mathbf{H}$ = numerical flux;
h = water depth;
l_k = Legendre polynomial of order k;
$\mathbf{n}$ = (n_1,n_2) unit outward normal vector;
R = matrix of right eigenvectors of $\mathbf{A}$;
t = time;
$\mathbf{U}$ = vector of conserved quantities;
$\mathbf{U_h^i}$ = solution approximation at time i;
$\hat{U}_k^i(t)$ = projection coefficients;
u,w = velocities in the x and y directions;
x,y = space coordinates;
α_k^i = Legendre coefficients;
(ξ_k,η_k) = Gauss-Legendre collocation nodes in reference square;

Λ = diagonal matrix whose entries are eigenvalues of **A**;
Φ = gh;
$\Psi_k(\mathbf{x})$ = polynomial basis; and
ω_k = Gauss-Legendre weights.

References

Abbot, M., Dansgaard, A., and Rodenhuis, G. (1973). "SYSTEM 21, 'Jupiter,' (a design system for two dimensional nearly horizontal flows)." *J. Hydraul. Res.*, 11, 1–28.

Alcrudo, F., and Garcia-Navarro, P. (1993). "A high-resolution Gudonov-type scheme in finite volumes for the 2-D shallow water equations." *Int. J. Numer. Methods Fluids*, 16(6), 489–505.

Ambrosi, D. (1995). "Approximation of shallow-water equations by Roe Riemann solver." *Int. J. Numer. Methods Fluids*, 20(2), 157–168.

Babuska, I., and Suri, M. (1994). "The P and H-P versions of the finite-element method, basic principles and properties." *SIAM Rev.*, 36(4), 578–632.

Bassi, F., and Rebay, S. (1997). "A high-order accurate discontinuous finite element method for the numerical solution of the compressible Navier-Stokes equations." *J. Comput. Phys.*, 131, 267–279.

Biswas, R., Devine, K. D., and Flaherty, J. E. (1994). "Parallel, adaptive, finite element methods for conservation laws." *Appl. Numer. Math.*, 14, 255–283.

Canuto, C., Hussaini, M. Y., Quarteroni, A., and Zang, T. A. (1988). *Spectral methods in fluid dynamics*, Springer, Berlin.

Cockburn, B., Karniadakis, G., Shu, C. W., and Griebel, M., eds. (2000), *Discontinuous Galerkin methods: Theory, computation and applications (lecture notes in computational science and engineering)*, Springer, Berlin.

Cockburn, B., and Shu, C. W. (1998). "The local discontinuous Galerkin method for time-dependent convection-diffusion systems." *SIAM (Soc. Ind. Appl. Math.) J. Numer. Anal.*, 35(6), 2440–2463.

Dronkers, J. J. (1964). *Tidal computations in rivers and coastal waters*, North-Holland, Amsterdam, The Netherlands.

Fennema, R. J., and Chaudhry, M. H. (1990). "Explicit methods for 2D transient free-surface flows." *J. Hydraul. Eng.*, 116(8), 1013–1034.

Fornberg, B. (1996). *A practical guide to pseudospectral methods*, Cambridge University Press, New York.

Fraccarollo, L., and Toro, E. F. (1995). "Experimental and numerical assessment of the shallow water model for two-dimensional dam-break type problems." *J. Hydraul. Res.*, 33(6), 843–864.

Harten, A., Lax, P. D., and van Leer, B. (1983). "On upstream differencing and Gudonov-type schemes for hyperbolic conservation-laws." *SIAM Rev.*, 25(1), 35–61.

Hirsch, C. (1989). *Numerical computation of internal and external flows, Vol. 1, Fundamentals of numerical discretization*, Wiley, New York.

Jha, A. K., Akiyama, J., and Ura, M. (1995). "First- and second-order flux difference splitting schemes for dam-break problem." *J. Hydraul. Eng.*, 121(12), 877–884.

Leendertse, J. (1967). "Aspects of a computational model for long-period water wave propagation." *Tech. Rep. RN-5294-PR*, Rand Corporation.

Majda, A., McDonough, J., and Osher, S. (1978). "The Fourier method for nonsmooth initial data." *Math. Comput.*, 32, 1041–1081.

Mingham, C. G., and Causon, D. M. (1998). "High-resolution finite-volume method for shallow water flows." *J. Hydraul. Eng.*, 124(6), 605–614.

Roe, P. L. (1981). "Approximate Riemann solvers, parameter vectors, and difference-schemes." *J. Comput. Phys.*, 43(2), 357–372.

Roe, P. L. (1985). "Some contributions to the modeling of discontinuous flows." *Lect. Appl. Math.*, 22, 163–193.

Schwanenberg, D., and Kongeter, J. (2000). "A discontinuous Galerkin method for the shallow water equations with source terms." *Discontinuous Galerkin Methods: Theory, Computation and Applications (Lecture Notes in Computational Science and Engineering)*, Cockburn, B., Karniadakis, G., Shu, C. W., and Griebel, M., eds., Springer, Berlin.

Shu, C. W., and Osher, S. (1988). "Efficient implementation of essentially non-oscillatory shock-capturing schemes." *J. Comput. Phys.*, 77, 439–471.

Stoker, J. J. (1957). *Water waves*, Interscience, New York.

Toro, E. F. (1989). "A weighted average flux method for hyperbolic conservation-laws." *Proc. R. Soc. London, Ser. A*, 423(1865), 401–418.

Toro, E. F. (1992). "Riemann problems and the WAF method for solving the two-dimensional shallow water equations." *Philos. Trans. R. Soc. London, Ser. A*, 338(1649), 43–68.

van Leer, B. (1974). "Towards the ultimate conservative difference scheme II: Monotonicity and conservation combined in a second order scheme." *J. Comput. Phys.*, 14, 361–370.

Wu, C., Huang, G., and Zheng, Y. (1999). "Theoretical solution of dam-break shock wave." *J. Hydraul. Eng.*, 125(11), 1210–1215.

Zhao, D. H., Shen, H. W., Tabios, G. Q., Lai, J. S., and Tan, W. Y. (1994). "Finite-volume two-dimensional unsteady-flow model for river basins." *J. Hydraul. Eng.*, 120(7), 863–883.

Zoppou, C., and Roberts, S. (2000). "Numerical solution of the two-dimensional unsteady dam break." *Appl. Math. Model.*, 24(7), 457–475.